

## Article

# Determination of Sr–Nd–Pb Isotopic Ratios of Rock Reference Materials Using Column Separation Techniques and TIMS

Hui Je Jo , Hyo Min Lee \*, Go-Eun Kim, Won Myung Choi and Taehoon Kim

Geoscience Platform Division, Korea Institute of Geoscience and Mineral Resources, 124 Gwahak-ro, Yuseong-gu, Daejeon 34132, Korea; jhj8218@kigam.re.kr (H.J.J.); goeun@kigam.re.kr (G.-E.K.); wmchoi@kigam.re.kr (W.M.C.); tkim@kigam.re.kr (T.K.)

\* Correspondence: hmlee@kigam.re.kr; Tel.: +82-42-868-3661

**Abstract:** Thermal ionization mass spectrometry (TIMS) can provide highly accurate strontium (Sr), neodymium (Nd), and lead (Pb) isotope measurements for geological and environmental samples. Traces of these isotopes are useful for understanding crustal reworking and growth. In this study, we conducted a sequential separation of Sr, Nd, and Pb and subsequently measured the  $^{87}\text{Sr}/^{86}\text{Sr}$ ,  $^{143}\text{Nd}/^{144}\text{Nd}$ ,  $^{206}\text{Pb}/^{204}\text{Pb}$ ,  $^{207}\text{Pb}/^{204}\text{Pb}$ , and  $^{208}\text{Pb}/^{204}\text{Pb}$  ratios of 13 widely used rock certified reference materials (CRMs), namely BCR-2, BHVO-2, GSP-2, JG-1a, HISS-1, Jlk-1, JSd-1, JSd-2, JSd-3, LKSD-1, MAG-1, SGR-1, and 4353A, using TIMS. In particular, we reported the first isotopic ratios of Sr, Nd, and Pb in 4353A, Sr and Nd in HISS-1 and SGR-1, and Sr in Jlk-1, JSd-2, JSd-3, and LKSD-1. The Sr–Nd–Pb isotopic compositions of most in-house CRMs were indistinguishable from previously reported values, although the Sr and Pb isotopic ratios of GSP-2, JSd-2, JSd-3, and LKSD-1 obtained in different aliquots and/or batches varied slightly. Hence, these rock reference materials can be used for monitoring the sample accuracy and assessing the quality of Sr–Nd–Pb isotope analyses.



**Citation:** Jo, H.J.; Lee, H.M.; Kim, G.-E.; Choi, W.M.; Kim, T. Determination of Sr–Nd–Pb Isotopic Ratios of Rock Reference Materials Using Column Separation Techniques and TIMS. *Separations* **2021**, *8*, 213. <https://doi.org/10.3390/separations8110213>

Academic Editor: Nico Ueberschaar

Received: 19 October 2021  
Accepted: 8 November 2021  
Published: 10 November 2021

**Publisher's Note:** MDPI stays neutral with regard to jurisdictional claims in published maps and institutional affiliations.



**Copyright:** © 2021 by the authors. Licensee MDPI, Basel, Switzerland. This article is an open access article distributed under the terms and conditions of the Creative Commons Attribution (CC BY) license (<https://creativecommons.org/licenses/by/4.0/>).

**Keywords:** separation chemistry; TIMS; Sr–Nd–Pb isotopes; rock reference material

## 1. Introduction

In geosciences, radiogenic isotopic ratios, combined with geochemical and stable isotope data, are used to determine the ages of terrestrial and extraterrestrial rocks and to understand geological processes and environments [1]. The daughter isotopes strontium (Sr) and neodymium (Nd) are produced by the decay of rubidium (Rb) and samarium (Sm), respectively. Radiometric Rb–Sr and Sm–Nd dating techniques are commonly used for silicate rock analysis because of the relatively long half-lives of parent isotopes. Lead (Pb) has four naturally occurring isotopes:  $^{208}\text{Pb}$ ,  $^{207}\text{Pb}$ ,  $^{206}\text{Pb}$ , and  $^{204}\text{Pb}$ . The former three isotopes are produced by the decay of thorium (Th) and uranium (U). Pb isotope systems are characterized by different decay chains, linked to the half-lives of parent isotopes and relatively large U–Th–Pb fractionations during geological processes. As members of radiogenic isotope systems, Sr, Nd, and Pb are abundant in the continental crust [2]. Numerous studies have clearly demonstrated the potential of radiogenic isotopes in terrestrial rocks to interpret the evolution of continental crust, the role of crustal and mantle interactions, supercontinent and orogenic cycles, and magmatic flare-ups [3–9]. Thus, the precise determination of Sr–Nd–Pb isotopic ratios is essential to understanding crustal reworking and growth. In addition, the importance of isotope analyses has been noted in a wide range of fields, such as environmental science, biology, archaeology, food traceability, and forensic investigations [10–16]. In particular, Pb isotopes, sometimes combined with Sr and Nd isotopes, have been used to effectively trace environmental metal pollution sources. Atmospheric Pb emissions are divided into trace amounts of natural emissions due to rock and/or mineral weathering and volcanic activity and abundant anthropogenic emissions due to large-scale fossil fuel combustion, mining, and smelting, which cause serious environmental pollution. Because Pb emissions change natural Pb

isotopic ratios, Pb isotope analysis is widely used to trace the origin and migration of pollutants in various fields, such as sediment [17–21], peat bog [22–24], ice and snow [25,26], soil [27,28], tree ring [29–31], and lichen [32–36].

In geochemical research, including age dating, crustal evolution, and tracing pollutant origins, isotopic ratios are measured using high-precision analysis equipment, such as thermal ionization mass spectrometry (TIMS) and multi-collector inductively coupled plasma mass spectrometry (MC-ICP-MS) equipped with a laser ablation system. Although advances in MC-ICP-MS have easily enabled measurements of Sr and Nd isotopic ratios, TIMS is the preferred method. The advantage of TIMS is that it produces lower and more consistent average instrumental mass fractionation (IMF), obtaining precise results using small amounts of samples and manually optimized evaporation and ionization of the elements of interest [37]. Isobaric ( $^{87}\text{Rb}$ ), monoatomic ( $^{86}\text{Kr}^+$ ), polyatomic ( $^{48}\text{Ca}^{40}\text{Ar}^+$ ), and molecular interferences in TIMS are relatively small and simple compared to with MC-ICP-MS [38–40]. To achieve reproducible and reliable Sr–Nd–Pb isotope data using TIMS, external reference materials (e.g., NIST SRM 987, JNdi-1, and NIST SRM 981) and certified geological materials are used to correct IMF and monitor analytical conditions, and chemical treatments and column chemistry are performed under clean conditions. For accurate isotope measurement, the high-purity separation of each element of interest is fundamental to prevent the interference from other elements. Therefore, it is important to determine the optimal element separation conditions, such as eluent type and concentration, resin type and particle size, and to increase the recovery rate. Generally, rock powders of certified reference materials (CRMs), distributed by the United States Geological Survey (USGS), the Geological Survey of Japan (GSJ), and the International Atomic Energy Agency (IAEA), are widely used. However, differences in Sr isotopic compositions have been found between new reference materials and their original counterparts [41]. This is probably caused by sample heterogeneity and contamination during sample, chemical, and analytical processing.

In this study, we conducted a sequential separation of Sr, Nd, and Pb, subsequently measured several aliquots of rock reference materials, investigated the reproducibility of this method in Sr–Nd–Pb isotope analyses, and determined the Sr–Nd–Pb isotopic ratios of in-house CRMs using TIMS.

## 2. Materials and Methods

The whole-rock Sr–Nd–Pb isotopic compositions of 13 powdered rock CRMs were measured. Basalts (BCR-2 and BHVO-2), granodiorite (GSP-2), marine mud (MAG-1), and shale (SGR-1) were obtained from the USGS. Another granodiorite sample (JG-1a) was obtained from the GSJ. Stream (JSd-1, JSd-2, and JSd-3), lake (JLk-1 and LKSD-1), and marine (HISS-1) sediments were obtained from the GSJ, the Canadian Certified Reference Material Programme, and the National Research Council. Lastly, rocky flats soil (4353A) was obtained from the IAEA. The geochemical processing of the samples and the Sr–Nd–Pb isotope analyses were carried out in the TIMS laboratory at the Korea Institute of Geoscience and Mineral Resources (KIGAM) in Daejeon, South Korea. Sample digestion and column chemistry were performed under conditions above the threshold of class 1000. The Sr–Nd–Pb isotopes were measured using TIMS (TRITON Plus, Thermo Fisher Scientific, Waltham, MA, USA) at the KIGAM.

### 2.1. Reagents, Labware, and Chromatographic Materials

Ultra-pure Milli-Q water (Millipore, Molsheim, France) with a resistivity of  $18.2 \text{ M}\Omega \text{ cm}^{-1}$  was used in all experiments. All chemicals used in this study were commercial products from Merck (Kenilworth, NJ, USA) and ODLAB (Gyeonggi, South Korea) without any further purification. Ultra-pure acids, namely hydrochloric acid (HCl), nitric acid ( $\text{HNO}_3$ ), and hydrofluoric acid (HF), were used for sample digestion and column chemistry. Supra-pure HCl and perchloric acid ( $\text{HClO}_4$ ) were only used for washing vials and resins and sample decomposition, respectively. Acid digestion was performed in pre-cleaned 60 mL

Savillex® screw-top Teflon perfluoroalkoxy (PFA) vessels (Eden Prairie, MN, USA). The element fractions were collected and dried in 7 and 15 mL PFA vials.

DOWEX® 50WX8 resin (hydrogen form, 100–200 mesh), manufactured by Merck, was reacted with cations and used to separate Pb, Sr, and rare earth elements (REEs). Ln resin, with a particle size of 100–150 µm and based on di-(2-ethylhexyl) orthophosphoric acid (HDEHP) in a pre-filter material (Eichrom Industries, Lyle, IL, USA), is commercially available and used for the purification of Nd. These resins must be pre-washed to remove impurities and organic components. After being cleaned three times with 6 M HCl and deionized water (DIW), the cationic and anionic exchange resins were poured into a self-designed quartz-glass column, which was 270 mm long with an inner diameter of 5 mm and a 30 mL reservoir (Figure 1). For the Pb purification, a 2 mL Poly-Prep® chromatography column (0.8 cm × 4 cm, a 10 mL reservoir; Bio-Rad, Hercules, CA, USA) and Eichrom extraction chromatographic Pb resin (100–150 µm) were used [42]. To remove impurities, the Pb resin was rinsed with 6 M HCl, 7 M HNO<sub>3</sub>, and DIW.

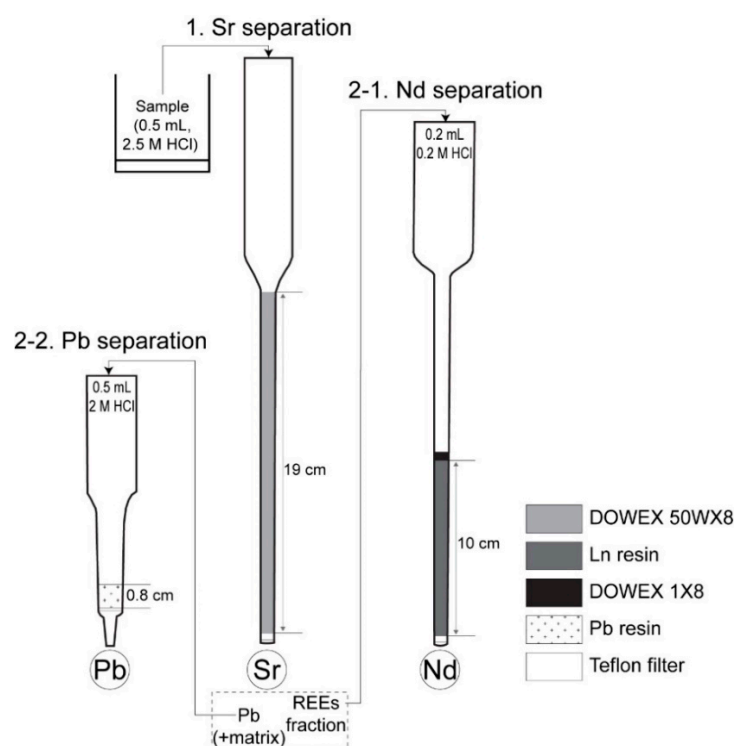


Figure 1. Sequential Sr–Nd–Pb separation chemistry.

### 2.2. Sample Digestion

The modified HF–HNO<sub>3</sub>–HClO<sub>4</sub>–HCl digestion method from [43] was applied for the decomposition of the rock samples. Approximately 100–200 mg of rock powder were weighed into 60 mL PFA vessels, followed by the addition of concentrated HF and HNO<sub>3</sub> (HF:HNO<sub>3</sub> = 2:1). The samples containing the HF–HNO<sub>3</sub> mixtures were sonicated in an ultrasonic bath for at least 15 min and heated on a hot plate at 160 °C for 2–3 days. The dissolved samples were dried overnight at 140 °C after the addition of 100–200 µL of concentrated HClO<sub>4</sub> to decompose the fluorides. Subsequently, 1 mL of concentrated HCl was added. The samples were again heated overnight at 160 °C and then dried at 110 °C. The samples were dissolved in 2–4 mL of 6 M HCl to check any remaining particles. Upon complete dissolution, the rock samples were finally dissolved using 0.5 mL of 2.5 M HCl.

### 2.3. Sr–Nd–Pb Separation

Before TIMS analysis, samples must be purified through ion-exchange. Table 1 presented the modified separation conditions of Sr and Nd from [44,45]. Before loading the sample solutions, the column and resin were pre-cleaned twice with 4 mL of 2.5 M HCl.

The 0.5 mL HCl solution obtained from the acid digestion was centrifuged at 13,000 rpm for 5 min and then transferred to a quartz-glass column packed with 4 mL of DOWEX<sup>®</sup> 50WX8 resin. The resin was subsequently washed with 0.5 mL of 2.5 M HCl, followed by 9.5 mL of 2.5 M HCl, to collect the Pb fraction. The resin was then rinsed with a further 13.5 mL of 2.5 M HCl to remove unnecessary matrix elements, particularly isobaric <sup>87</sup>Rb. The Sr fraction was eluted with 5.5 mL of 2.5 M HCl. The resin was then rinsed with 2 mL of 2.5 M HCl, followed by 1 mL of 6 M HCl to elute REEs. Finally, the REEs fraction was collected in 10 mL of 6 M HCl. To separate Nd using the Ln resin method [45], a sample solution including REEs was prepared by keeping the samples in 0.2 mL of 0.25 M HCl. A quartz-glass column was pre-cleaned with 4 mL 0.25 M HCl and packed with 2 mL of Ln (HDEHP) resin, after which the sample solution was passed through the column. The residues were rinsed with 7.3–7.5 mL 0.25 M HCl, depending on the Nd concentration. Then, Nd was collected with 3.5–3.7 mL of 0.25 M HCl. Upon completing the exchange chromatography, the cationic resin was cleaned successively with 6 M HCl, DIW, and 2.5 M HCl, and the anionic exchange resin was cleaned successively with 6 M HCl and 0.25 M HCl. The Sr and Nd fractions were further purified using concentrated HNO<sub>3</sub>.

Generally, two rounds of element separation using hydrogen bromide (HBr) are required to perform TIMS Pb isotope analysis. However, despite high analytical reproducibility and low analytical error of this separation method, the pre-treatment process is time-consuming, and the required ultra-pure HBr is difficult to obtain commercially in South Korea. To solve this problem, we attempted to establish a simple and efficient method for separating Pb using HCl and Eichrom's extraction chromatography Pb resin [42]. Before the Pb separation, 10.5 mL of the 2.5 M HCl solution collected from cation column chemistry were dried, followed by the addition of 0.5 mL of 2 M HCl. The column and the resin were pre-cleaned and conditioned using 6 M and 2 M HCl. The 0.5 mL HCl sample solution was transferred to a Poly-Prep<sup>®</sup> chromatography column packed with 0.4 mL of Pb resin. After washing with 4.5 mL of 2 M HCl, the Pb fraction was eluted with 2 mL of 8 M HCl. The column and resin were cleaned using 6 M HCl and DIW. The Pb sample was further purified using concentrated HNO<sub>3</sub> and 0.1 M phosphoric acid (H<sub>3</sub>PO<sub>4</sub>). Detailed column conditions and procedures for Pb separation are described in [42].

**Table 1.** Sr–Nd purification procedures.

Step	Eluting Reagent	Eluting Volume (mL)
Sr, Pb, and rare earth elements (REEs) separation (4 mL of DOWEX 50WX8 resin)		
Cleaning column	2.5 M HCl	4 × 2
Loading sample <sup>1</sup>	2.5 M HCl	0.5
Rinsing <sup>1</sup>	2.5 M HCl	0.5
Eluting Pb	2.5 M HCl	9.5
Rinsing	2.5 M HCl	13.5
Eluting Sr	2.5 M HCl	5.5
Rinsing	2.5 M HCl	2
Rinsing	6 M HCl	1
Eluting REEs	6 M HCl	10
Cleaning column	6 M HCl	30
Cleaning column	DIW	30
Cleaning column	2.5 M HCl	8
Nd separation (2 mL of Ln resin)		
Cleaning column	0.25 M HCl	2 × 2
Loading sample	0.25 M HCl	0.2
Rinsing	0.25 M HCl	0.2
Rinsing	0.25 M HCl	7.5–7.3
Eluting Nd	0.25 M HCl	3.5–3.7
Cleaning column	6 M HCl	30
Cleaning column	0.25 M HCl	30

<sup>1</sup> The solution was collected for Pb separation.

### 2.4. TIMS Sr–Nd–Pb Isotope Analyses

Sr–Nd–Pb isotope measurements were conducted using a TRITON Plus TIMS instrument equipped with nine Faraday detectors and one ion counter. All Faraday cups with a  $10^{11}\text{-}\Omega$  resistor were sequentially connected to all amplifiers to cancel the gain factor uncertainties by using amplifier rotation. Therefore, this technique can achieve low-ppm external reproducibility. Pre-degassed filaments with welded tantalum (Ta) were used for Sr isotope analysis, while rhenium (Re) ribbons (0.035 mm thick, 0.77 mm wide, and 99.98% pure; H. Cross Company) were used for Nd and Pb analyses. Raw Sr and Nd data were collected in multi-dynamic collection mode. The collector arrays are presented in Table 2.

**Table 2.** Cup configuration for Sr–Nd–Pb isotope analysis.

Element	L4	L3	L2	L1	Ax	H1	H2	H3	H4
Sr				$^{84}\text{Sr}$	$^{85}\text{Rb}$	$^{86}\text{Sr}$	$^{87}\text{Sr}$	$^{88}\text{Sr}$	
Nd	$^{140}\text{Ce}$	$^{142}\text{Nd}$	$^{143}\text{Nd}$	$^{144}\text{Nd}$	$^{145}\text{Nd}$	$^{146}\text{Nd}$	$^{147}\text{Sm}$	$^{148}\text{Nd}$	$^{150}\text{Nd}$
Pb					$^{204}\text{Pb}$	$^{206}\text{Pb}$	$^{207}\text{Pb}$	$^{208}\text{Pb}$	

During the Sr isotope analysis, the purified Sr sample, dissolved in 1  $\mu\text{L}$  of DIW, was transferred onto a single Ta filament with 1 M  $\text{H}_3\text{PO}_4$  to stimulate strong emission. The suitable ionization temperature for TIMS Sr measurements is 1350–1400  $^\circ\text{C}$ , depending on the sample. When the  $^{88}\text{Sr}$  ion beam intensity reached approximately 1 V in the Faraday cup, data acquisition was performed using the static multiple Faraday cup mode. Each run consisted of 10 blocks of 20 cycles each. The  $^{87}\text{Sr}/^{86}\text{Sr}$  ratio was corrected for IMF and normalized by the  $^{86}\text{Sr}/^{88}\text{Sr}$  ratio of 0.1194 using an exponential law. During the analytical period, the replicate analyses of NIST SRM 987 yielded an average  $^{87}\text{Sr}/^{86}\text{Sr}$  ratio of  $0.710268 \pm 0.000003$  ( $n = 10$ , 1 standard deviation (SD); Figure 2a and Table 3). This result agreed with a previously reported value within the error range [46].

**Table 3.** TIMS results for NIST SRM 987 and JNdi-1.

Sample Number	$^{87}\text{Sr}/^{86}\text{Sr}$	2 $\sigma$ SE	$n$	$^{143}\text{Nd}/^{144}\text{Nd}$	2 $\sigma$ SE	$n$
	NIST SRM 987			JNdi-1		
190723	0.710266	0.000005	20	0.512100	0.000002	20
191111	0.710271	0.000003	20	0.512102	0.000003	20
191212	0.710271	0.000003	20	0.512102	0.000003	20
200520	0.710266	0.000003	20	0.512101	0.000001	20
200716	0.710264	0.000003	20	0.512100	0.000002	20
200806	0.710264	0.000003	20	0.512100	0.000003	20
210415	0.710270	0.000003	20	0.512103	0.000002	20
210512	0.710270	0.000003	20	0.512103	0.000002	20
210628	0.710266	0.000006	20	0.512101	0.000002	20
210911	0.710269	0.000003	20	0.512100	0.000002	20

During the Nd isotope analysis, the Nd fraction, dissolved in 1  $\mu\text{L}$  of DIW, was transferred onto double-Re filaments with 0.1 M  $\text{H}_3\text{PO}_4$ . An ionization temperature of 1650–1700  $^\circ\text{C}$  is desirable for TIMS Nd measurements. Data were acquired using the static multiple Faraday cup mode with a mass  $^{144}\text{Nd}$  ion beam intensity of 1 V and a run consisting of 18 blocks of 10 cycles each. The  $^{143}\text{Nd}/^{144}\text{Nd}$  ratio was normalized by a  $^{146}\text{Nd}/^{144}\text{Nd}$  ratio of 0.7219 using an exponential law. The replicate analyses of JNdi-1 gave an average  $^{143}\text{Nd}/^{144}\text{Nd}$  ratio of  $0.512101 \pm 0.000001$  ( $n = 10$ , 1 SD), which is indistinguishable from previously reported values of 0.512070–0.512129 (Figure 2b and Table 3).

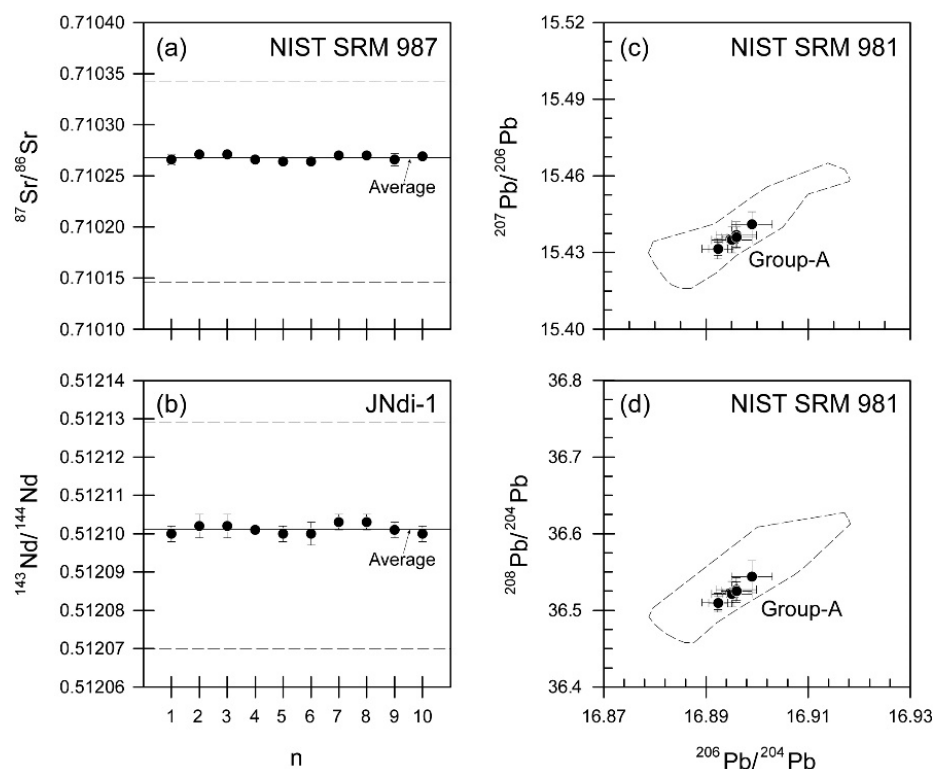


**Figure 2.** Replicate measurements of NIST SRM 987 for the Sr isotope (a) and JNdi-1 for Nd isotope (b) with the average (solid line) and the range (dashed lines) of the literature data from the GeoReM database (<http://georem.mpch-mainz.gwdg.de/>, accessed 1 October 2021). Plots of  $^{207}\text{Pb}/^{204}\text{Pb}$  vs.  $^{206}\text{Pb}/^{204}\text{Pb}$  ratios (c) and  $^{208}\text{Pb}/^{204}\text{Pb}$  vs.  $^{206}\text{Pb}/^{204}\text{Pb}$  ratios (d) showing the results obtained for NIST SRM 981 in a previous study [42] and this study. The dashed areas represent the range of Pb isotopic compositions of Group-A, obtained from [47].

During the Pb isotope analysis, the Pb sample, dissolved in 1  $\mu\text{L}$  of DIW, was transferred onto a single-Re filament with a silica gel and 0.1 M  $\text{H}_3\text{PO}_4$ . Depending on the silica gel, an ionization temperature of 1200–1250  $^\circ\text{C}$  is preferable for TIMS Pb measurements. Data were acquired using the static multiple Faraday cup mode, with a  $^{208}\text{Pb}$  ion beam intensity of approximately 3 V and a run consisting of 4 blocks of 10 cycles each. Unfortunately, internal calibration was not available for Pb analysis because only  $^{204}\text{Pb}$  was non-radiogenic among the four Pb isotopes. This can be corrected by using double spikes, but it is not widely used because it is difficult to obtain commercially in South Korea. Therefore, external calibration was applied to the mass fractionation generated during analysis by measuring the Pb isotopic ratios of NIST SRM 981. Replicate analyses of NIST SRM 981 yielded  $^{206}\text{Pb}/^{204}\text{Pb}$ ,  $^{207}\text{Pb}/^{204}\text{Pb}$ , and  $^{208}\text{Pb}/^{204}\text{Pb}$  ratios of  $16.894 \pm 0.002$ ,  $15.434 \pm 0.002$ , and  $36.518 \pm 0.008$  ( $n = 5$ , 1 SD), respectively, which are consistent with those reported in [47] (Figure 2c,d and Table 4). The total procedural blank levels of Sr, Nd, and Pb were below ca. 300, 50, and 200 pg, respectively.

**Table 4.** TIMS results for NIST SRM 981.

Sample Number	$^{206}\text{Pb}/^{204}\text{Pb}$	$2\sigma$ SE	$^{207}\text{Pb}/^{204}\text{Pb}$	$2\sigma$ SE	$^{208}\text{Pb}/^{204}\text{Pb}$	$2\sigma$ SE	$n$
200716	16.895	0.001	15.435	0.002	36.522	0.005	5
200806	16.895	0.004	15.435	0.005	36.521	0.017	5
210512	16.892	0.003	15.431	0.004	36.510	0.012	10
210628	16.892	0.002	15.431	0.003	36.510	0.008	10
210911	16.896	0.004	15.437	0.005	36.527	0.016	10

### 3. Results and Discussion

In contrast to the basalt samples, the granodiorite (GSP-2 and JG-1a) and sedimentary (JLk-1, JSd-3, LKSD-1, MAG-1, SGR-1, and 4353A) samples had difficulties in completely decomposing with an acid mixture of HF–HNO<sub>3</sub>–HClO<sub>4</sub>–HCl. In most cases, a small amount of black particles remained. To compensate for the uncertainty in the geochemical and isotope data, complete recovery and sample homogeneity are required. However, it is difficult to completely recover trace elements in felsic and mafic rocks because of the presence of hard-to-digest minerals and co-precipitated insoluble fluoride [43,48]. Rock samples from outcrops are also easily contaminated and altered. Pretorius et al. [49] found that some granitoid samples show the poorer reproducibility of elemental concentrations because of the inhomogeneous distribution of elements. Fortunately, a Sr–Nd–Pb isotope equilibrium between the sample solution and suspended particles was mostly attained.

During the separation protocol, there were elution overlaps between Sr and Rb and between Nd and Ce (see Figure I–4 from [44] and Figure 4 from [45]), but no overlap was found between Sr, Nd, and Pb. Because of the peak overlapping and tailing, the Sr and Nd solutions had isobaric interferences such as <sup>87</sup>Rb and <sup>143</sup>(CeH)<sup>+</sup> [38–40,50]. However, these Rb and Ce interferences were not ionized under the TIMS Sr and Nd measurement conditions. Therefore, this separation protocol is not suitable for the Sr–Nd isotope analysis of geological and environmental samples with high Rb and Ce concentrations using MC-ICP-MS. To determine whether the Pb separation method affects the isotopic ratio [42], Pb isotopic ratios were measured by separating NIST SRM 981 in the same way as the standard rock sample. The Pb isotopic ratios (<sup>206</sup>Pb/<sup>204</sup>Pb, <sup>207</sup>Pb/<sup>204</sup>Pb, and <sup>208</sup>Pb/<sup>204</sup>Pb) agreed with those without Pb separation within the error range. This means that the conditions of the experimental environment, including DIW, reagents, containers, and acid-resistant clean laboratory used for Pb separation experiments, are also suitable for Pb isotope analysis.

The Sr and Nd isotopic compositions of the 13 rock CRMs are shown in Table 5. To our knowledge, we have presented the first Sr isotope data for JSd-2, JSd-3, HISS-1, JLk-1, LKSD-1 SGR-1, and 4353A and the first Nd isotope data for HISS-1, SGR-1, and 4353A. All errors are given as 2σ standard errors (SE). Typically, the internal precision of every run of Sr and Nd isotope measurements was less than 20 ppm. The Sr and Nd isotopic compositions of the two basalt samples strongly agreed with the literature data given in the GeoReM database. The Sr and Nd isotopic ratios of BCR-2 measured in this study were  $0.705022 \pm 0.000011$  ( $n = 5$ , 1 SD) and  $0.512628 \pm 0.000003$  ( $n = 5$ , 1 SD), respectively. The Sr and Nd isotope analyses of BHVO-2 yielded a <sup>87</sup>Sr/<sup>86</sup>Sr ratio of  $0.703487 \pm 0.000003$  ( $n = 4$ , 1 SD) and a <sup>143</sup>Nd/<sup>144</sup>Nd ratio of  $0.512974 \pm 0.000006$  ( $n = 4$ , 1 SD). The different sample aliquots of GSP-2 showed small variations in <sup>87</sup>Sr/<sup>86</sup>Sr ratios, ranging from 0.765019 to 0.765212 with an average of  $0.765143 \pm 0.00054$  ( $n = 10$ , 1 SD). It is possible that this was caused by sample heterogeneity and/or incomplete recovery. By contrast, Nd isotopic compositions were considerably more homogeneous, with an average of  $0.511359 \pm 0.000003$  ( $n = 10$ , 1 SD). Four Sr–Nd isotope measurements for JG-1a yielded the average <sup>87</sup>Sr/<sup>86</sup>Sr and <sup>143</sup>Nd/<sup>144</sup>Nd ratios of  $0.710984 \pm 0.000008$  (1 SD) and  $0.512372 \pm 0.000004$  (1 SD), respectively. The respective isotopic ratios of <sup>87</sup>Sr/<sup>86</sup>Sr and <sup>143</sup>Nd/<sup>144</sup>Nd obtained for HISS-1 were  $0.712681 \pm 0.000009$  (2σ SE) and  $0.511844 \pm 0.000006$  (2σ SE). Two Sr–Nd measurements of MAG-1 yielded an average <sup>87</sup>Sr/<sup>86</sup>Sr ratio of  $0.722747 \pm 0.000023$  (1 SD) and an average <sup>143</sup>Nd/<sup>144</sup>Nd ratio of  $0.512059 \pm 0.000004$  (1 SD), which are in line with the previously reported TIMS ratios within the error range [51]. The <sup>87</sup>Sr/<sup>86</sup>Sr and <sup>143</sup>Nd/<sup>144</sup>Nd ratios of the three stream sediments (JSd-1, JSd-2, and JSd-3) ranged from 0.705732 to 0.731407 and from 0.511970 to 0.512640, respectively. The respective Sr and Nd isotopic ratios of the two lake sediments (JLk-1 and LKSD-1) ranged from 0.709773 to 0.721863 and from 0.512134 to 0.512173. The results of the TIMS Nd measurements in stream and lake sediments were within the range reported in previous studies [51,52]. The <sup>87</sup>Sr/<sup>86</sup>Sr and <sup>143</sup>Nd/<sup>144</sup>Nd isotopic ratios of SGR-1 were  $0.712139 \pm 0.000011$  (2σ SE) and  $0.512003 \pm 0.000005$  (2σ SE), respectively. Lastly, seven Sr–Nd measurements for

4353A yielded average  $^{87}\text{Sr}/^{86}\text{Sr}$  and  $^{143}\text{Nd}/^{144}\text{Nd}$  ratios of  $0.730442 \pm 0.000017$  (1 SD) and  $0.511782 \pm 0.000005$  (1 SD), respectively. Although each sedimentary rock sample had slightly heterogeneous Sr isotopic compositions, their Nd isotopic compositions were relatively constant. The percent-relative SD of isotopic values measured across the various rock CRMs was less than  $\pm 0.005\%$  for the Nd isotope and  $\pm 0.01\%$  for the Sr isotope, although some Sr isotope results of GSP-2 and MAG-1 showed slightly higher SD (Figure 3).

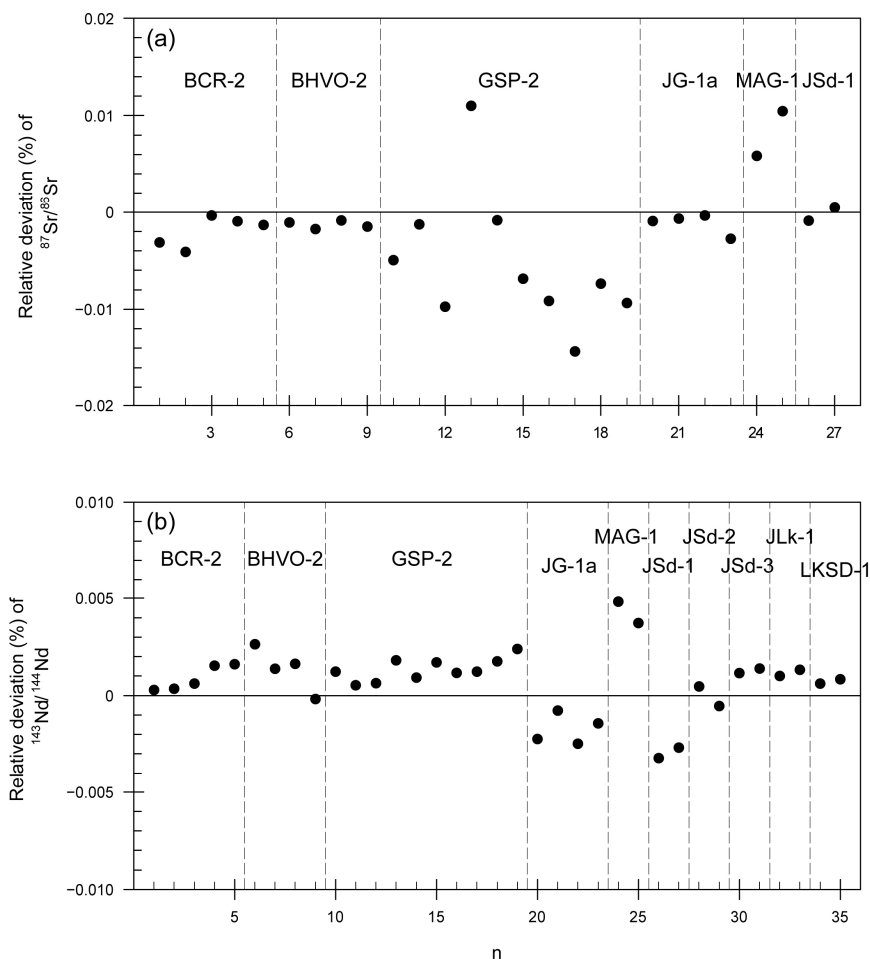


**Figure 3.** Comparison between the measured and certified ratios of  $^{87}\text{Sr}/^{86}\text{Sr}$  (a) and  $^{143}\text{Nd}/^{144}\text{Nd}$  (b) of rock CRMs. To calculate the average, the Sr and Nd isotopic compositions of CRMs were taken from the GeoReM database. Relative deviation (%) =  $(1 - \text{measured value}/\text{certified value}) \times 100\%$ .

**Table 5.** Sr–Nd isotopic compositions of rock CRMs.

Sample Number <sup>1</sup>	$^{87}\text{Sr}/^{86}\text{Sr}$	$2\sigma$ SE	$^{143}\text{Nd}/^{144}\text{Nd}$	$2\sigma$ SE
<u>BCR-2 (xxx)</u>				
1911	0.705030	0.000011	0.512631	0.000005
2005	0.705037	0.000010	0.512631	0.000008
2007	0.705011	0.000011	0.512629	0.000006
2008-1	0.705015	0.000009	0.512624	0.000007
2008-2	0.705018	0.000009	0.512624	0.000008
<u>BHVO-2 (xxx)</u>				
1411 <sup>2</sup>	0.703485	0.000014	0.512968	0.000012
1911	0.703490	0.000010	0.512974	0.000007
2008	0.703484	0.000010	0.512973	0.000007
2108	0.703488	0.000010	0.512982	0.000007

Table 5. Cont.

Sample Number <sup>1</sup>	<sup>87</sup> Sr/ <sup>86</sup> Sr	2σ SE	<sup>143</sup> Nd/ <sup>144</sup> Nd	2σ SE
<u>GSP-2 (xxx)</u>				
1907	0.765141	0.000010	0.511360	0.000006
1911	0.765113	0.000010	0.511364	0.000006
1912	0.765177	0.000009	0.511363	0.000006
2005	0.765019	0.000009	0.511357	0.000006
2007	0.765109	0.000009	0.511362	0.000006
2008	0.765155	0.000011	0.511358	0.000008
<u>GSP-2 (599)</u>				
2005	0.765173	0.000010	0.511360	0.000007
2007	0.765212	0.000011	0.511360	0.000006
<u>GSP-2 (1273)</u>				
2005	0.765159	0.000009	0.511357	0.000006
2007	0.765174	0.000010	0.511354	0.000007
<u>JG-1a (xxx)</u>				
1907	0.710982	0.000010	0.512375	0.000007
1911	0.710981	0.000010	0.512368	0.000007
2008	0.710978	0.000009	0.512376	0.000007
2103-1	0.710995	0.000009	0.512371	0.000006
<u>HISS-1 (xxx)</u>				
2108	0.712681	0.000009	0.511844	0.000006
<u>MAG-1 (16)</u>				
2106	0.722763	0.000008	0.512056	0.000006
2108	0.722730	0.000009	0.512061	0.000007
<u>Jsd-1 (xxx)</u>				
2106	0.705741	0.000009	0.512581	0.000005
2108	0.705732	0.000009	0.512578	0.000007
<u>Jsd-2 (xxx)</u>				
2106	0.706929	0.000010	0.512635	0.000007
2108	0.706926	0.000009	0.512640	0.000007
<u>Jsd-3 (xxx)</u>				
2106	0.731407	0.000009	0.511971	0.000007
2108	0.731228	0.000010	0.511970	0.000007
2109	0.731294	0.000018		
<u>JLk-1 (8)</u>				
2106	0.721840	0.000009	0.512135	0.000006
2108	0.721863	0.000009	0.512134	0.000006
<u>LKSD-1 (1549)</u>				
2106	0.709773	0.000013	0.512173	0.000008
2108	0.709806	0.000009	0.512172	0.000007
2109	0.709780	0.000009		
<u>SGR-1 (10)</u>				
2106	0.712139	0.000011	0.512003	0.000005
<u>4353A (xxx)</u>				
2106	0.730460	0.000008	0.511776	0.000006
2108-1	0.730415	0.000010	0.511793	0.000007
2108-2	0.730460	0.000010	0.511780	0.000007
2109-1	0.730451	0.000008	0.511783	0.000008
2109-2	0.730438	0.000010	0.511780	0.000007
2109-3	0.730432	0.000010	0.511778	0.000008
2109-4	0.730439	0.000010	0.511784	0.000008

<sup>1</sup> Batch or split numbers are in parentheses. xxx represents the sample without a batch number. <sup>2</sup> Sr–Nd isotope data are from [53].

Eight reference materials were selected to measure Pb isotopic compositions using TIMS, the results of which are shown in Table 6. The Pb isotopic compositions of 4353A are presented first. Six Pb analyses of GSP-2 yielded average <sup>206</sup>Pb/<sup>204</sup>Pb, <sup>207</sup>Pb/<sup>204</sup>Pb, and <sup>208</sup>Pb/<sup>204</sup>Pb ratios of 17.595 ± 0.032 (1 SD), 15.508 ± 0.017 (1 SD), and 51.261 ± 0.377 (1 SD), respectively. The Pb isotopic ratios of JG-1a were as follows: <sup>206</sup>Pb/<sup>204</sup>Pb ratio,

18.613 ± 0.008 (*n* = 2, 1 SD); <sup>207</sup>Pb/<sup>204</sup>Pb ratio, 15.624 ± 0.001 (*n* = 2, 1 SD); and <sup>208</sup>Pb/<sup>204</sup>Pb ratio, 38.782 ± 0.041 (*n* = 2, 1 SD). The Pb isotopic compositions measured in the two granodiorite samples agreed strongly with the published values given in the GeoReM database. The <sup>206</sup>Pb/<sup>204</sup>Pb, <sup>207</sup>Pb/<sup>204</sup>Pb, and <sup>208</sup>Pb/<sup>204</sup>Pb ratios of MAG-1 and JSd-1 are as well in agreement with the previously reported values [51,52,54]. The averages of the <sup>207</sup>Pb/<sup>204</sup>Pb and <sup>208</sup>Pb/<sup>204</sup>Pb ratios obtained for JSd-2, JSd-3, and LKSD-1 in this study were slightly higher than those obtained from the MC-ICP-MS analysis [52]. In contrast to JSd-1 and JSd-2, JSd-3 and LKSD-1 were difficult to completely dissolve using the acid digestion method. Révillon and Hureau-Mazaudier [55] recommended the Parr bombs digestion method, using HClO<sub>4</sub> and HF, for the complete decomposition of sediment samples. However, the geochemical results from [52] suggested that the inhomogeneous sample powder and a relatively large sample grain size could be attributed to the large bias of elemental and isotopic compositions. In the case of JG-1a, which has a granodiorite composition, the Pb isotopic ratios exhibited a broader range than those of Sr and Nd (Figures 3 and 4) [56–58]. Five Pb analyses of 4353A yielded average <sup>206</sup>Pb/<sup>204</sup>Pb, <sup>207</sup>Pb/<sup>204</sup>Pb, and <sup>208</sup>Pb/<sup>204</sup>Pb ratios of 19.094 ± 0.015 (1 SD), 15.681 ± 0.014 (1 SD), and 39.722 ± 0.053 (1 SD), respectively. Excluding some data from GSP-2 and JSd-2, the relative deviation of Pb isotopic ratios across all rock CRMs was less than ± 0.5% for <sup>206</sup>Pb/<sup>204</sup>Pb and <sup>207</sup>Pb/<sup>204</sup>Pb ratios, and ± 1% for <sup>208</sup>Pb/<sup>204</sup>Pb ratios (Figure 4). Overall, the Sr–Nd–Pb isotopic compositions of rock CRMs obtained in this study using acid digestion, column chemistry, and TIMS analyses agree strongly with the literature (see the GeoReM online database, accessed 1 October 2021).

**Table 6.** Pb isotopic compositions of rock CRMs.

Sample Number	<sup>206</sup> Pb/ <sup>204</sup> Pb	2σ SE	<sup>207</sup> Pb/ <sup>204</sup> Pb	2σ SE	<sup>208</sup> Pb/ <sup>204</sup> Pb	2σ SE
<u>GSP-2 (xxx)</u>						
2005	17.576	0.001	15.507	0.001	50.837	0.002
2007	17.647	0.001	15.541	0.001	51.528	0.003
<u>GSP-2 (599)</u>						
2005	17.558	0.001	15.503	0.001	50.870	0.002
2007	17.587	0.001	15.489	0.001	51.677	0.003
<u>GSP-2 (1273)</u>						
2005	17.616	0.001	15.504	0.001	51.576	0.003
2007	17.584	0.001	15.506	0.001	51.078	0.003
<u>JG-1a (xxx)</u>						
2103-1	18.619	0.001	15.625	0.001	38.753	0.002
2103-2	18.607	0.002	15.623	0.002	38.811	0.004
<u>MAG-1 (16)</u>						
2106	18.871	0.002	15.668	0.002	38.867	0.007
2109	18.862	0.002	15.650	0.002	38.804	0.004
<u>JSd-1 (xxx)</u>						
2106	18.480	0.003	15.614	0.002	38.597	0.006
2109	18.496	0.002	15.634	0.002	38.665	0.004
<u>JSd-2 (xxx)</u>						
2106	18.162	0.003	15.681	0.003	38.447	0.007
2109	18.163	0.009	15.665	0.008	38.412	0.019
<u>JSd-3 (xxx)</u>						
2106	18.418	0.003	15.697	0.003	39.054	0.007
2109	18.404	0.003	15.680	0.002	38.999	0.006
<u>LKSD-1 (1549)</u>						
2106	18.326	0.001	15.640	0.001	38.102	0.004
2109	18.361	0.011	15.647	0.010	38.220	0.023
<u>4353A (xxx)</u>						
2106	19.089	0.001	15.681	0.001	39.721	0.003
2109-1	19.070	0.002	15.658	0.001	39.638	0.003
2109-2	19.105	0.003	15.693	0.002	39.768	0.006
2109-3	19.106	0.002	15.694	0.002	39.764	0.005
2109-4	19.100	0.002	15.679	0.002	39.717	0.004

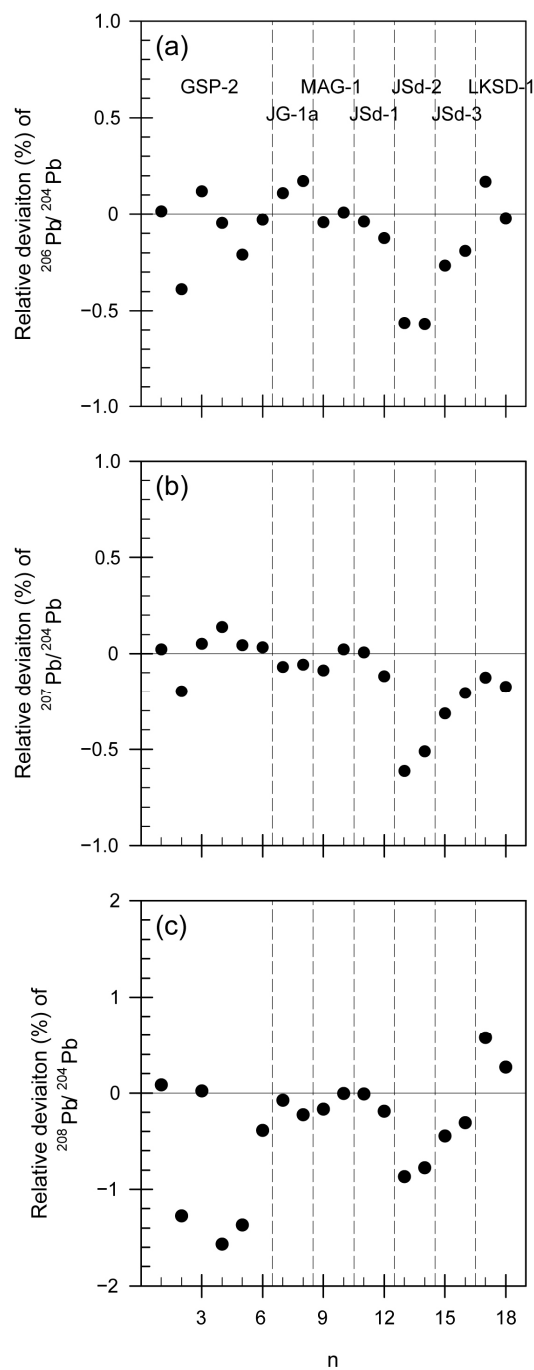


**Figure 4.** Comparison between the measured and certified  $^{206}\text{Pb}/^{204}\text{Pb}$  (a),  $^{207}\text{Pb}/^{204}\text{Pb}$  (b), and  $^{208}\text{Pb}/^{204}\text{Pb}$  (c) ratios of rock CRMs. To calculate the average, the Pb isotopic compositions of CRMs were taken from the GeoReM database. Relative deviation (%) =  $(1 - \text{measured value}/\text{certified value}) \times 100\%$ .

#### 4. Conclusions

In this study, Sr–Nd–Pb isotopic compositions were measured in 13 geological reference materials, such as basalt, granodiorite, shale, and sediments (marine mud and soil) using TIMS at the KIGAM. Although some Sr and Pb isotopic compositions of CRMs (GSP-2, JSd-2, JSd-3, and LKSD-1) varied slightly, the Sr–Nd–Pb isotopic compositions of most reference materials corresponded well with previously reported values within the error range. Furthermore, we presented the first Sr–Nd–Pb isotopic ratios of several reference materials (JSd-2, JSd-3, HISS-1, Jlk-1, LKSD-1, SGR-1, and 4353A). Therefore, these can be used as in-house reference materials to verify the performance of instruments

and validate Sr, Nd, and Pb isotopes in unknown geological and environmental samples. The combination of sample treatments, separation methods, and TIMS measurements used in this study also achieved high internal precisions of less than 20 ppm for  $^{87}\text{Sr}/^{86}\text{Sr}$  ratios and less than 10 ppm for  $^{143}\text{Nd}/^{144}\text{Nd}$  ratios.

**Author Contributions:** Conceptualization, methodology, and investigation, H.J.J., H.M.L., and T.K.; resources, G.-E.K. and W.M.C.; data curation, H.J.J. and H.M.L.; writing—original draft preparation, H.J.J. and H.M.L.; writing—review and editing, H.J.J. and H.M.L.; visualization, H.J.J. and H.M.L.; funding acquisition, H.M.L. All authors have read and agreed to the published version of the manuscript.

**Funding:** This work was supported by grants from the Korea Institute of Geoscience and Mineral Resources (GP2020-019).

**Institutional Review Board Statement:** Not applicable.

**Informed Consent Statement:** Not applicable.

**Data Availability Statement:** Data available in a publicly accessible repository.

**Acknowledgments:** We thank Sanghee Park at the Korea Basic Science Institute for the help with the experimental setup of Pb separation. We also thank two anonymous reviewers for their help in improving the manuscript.

**Conflicts of Interest:** The authors declare no conflict of interest.

## References

1. Faure, G.; Mensing, T.A. *Isotopes: Principles and Applications*, 3rd ed.; John Wiley & Sons, Inc.: New York, NY, USA, 2005; p. 897.
2. Rudnick, R.L.; Gao, S. Composition of the continental crust. In *The Crust*; Rudnick, R.L., Ed.; Elsevier: Amsterdam, The Netherlands, 2003; Volume 3, pp. 1–64.
3. Dhuime, B.; Wuestefeld, A.; Hawkesworth, C.J. Emergence of modern continental crust about 3 billion years ago. *Nat. Geosci.* **2015**, *8*, 552–555. [[CrossRef](#)]
4. Hawkesworth, C.J.; Cawood, P.A.; Dhuime, B.; Kemp, T.I.S. Earth's Continental Lithosphere through Time. *Annu. Rev. Earth Planet Sci.* **2017**, *45*, 169–198. [[CrossRef](#)]
5. Gao, S.; Rudnick, R.L.; Yuan, H.; Liu, X.; Liu, Y.; Xu, W.; Ling, W.; Ayers, J.; Wang, X.; Wang, Q. Recycling lower continental crust in the North China craton. *Nature* **2004**, *432*, 892–897. [[CrossRef](#)] [[PubMed](#)]
6. Chauvel, C.; Lewin, E.; Carpentier, M.; Arndt, N.T.; Marini, J.C. Role of recycled oceanic basalt and sediment in generating the Hf–Nd mantle array. *Nat. Geosci.* **2008**, *1*, 64–67. [[CrossRef](#)]
7. Spencer, C.J.; Murphy, J.B.; Kirkland, C.L.; Liu, Y.; Mitchell, R.N. A Palaeoproterozoic tectono-magmatic lull as a potential trigger for the supercontinent cycle. *Nat. Geosci.* **2018**, *11*, 97–101. [[CrossRef](#)]
8. Chapman, J.B.; Ducea, M.N. The role of arc migration in Cordilleran orogenic cyclicity. *Geology* **2019**, *47*, 627–631. [[CrossRef](#)]
9. Ducea, M.N.; Barton, M.D. Igniting flare-up events in Cordilleran arcs. *Geology* **2007**, *35*, 1047–1050. [[CrossRef](#)]
10. Slovak, N.M.; Paytan, A. Application of Sr isotopes in archaeology. In *Handbook of Environmental Isotope Geochemistry*; Baskaran, M., Ed.; Springer: Berlin/Heidelberg, Germany, 2012; Volume 1, pp. 743–768.
11. Font, L.; Jonker, G.; van Aalderen, P.A.; Schiltmans, E.F.; Davies, G.R. Provenancing of unidentified World War II casualties: Application of strontium and oxygen isotope analysis in tooth enamel. *Sci. Justice* **2015**, *55*, 10–17. [[CrossRef](#)]
12. Coelho, I.; Castanheira, I.; Bordado, J.M.; Donard, O.; Silva, J.A.L. Recent developments and trends in the application of strontium and its isotopes in biological related fields. *TrAC-Trends Anal. Chem.* **2017**, *90*, 45–61. [[CrossRef](#)]
13. Crowley, B.E.; Miller, J.H.; Bataille, C.P. Strontium isotopes ( $^{87}\text{Sr}/^{86}\text{Sr}$ ) in terrestrial ecological and palaeoecological research: Empirical efforts and recent advances in continental-scale models. *Biol. Rev.* **2017**, *92*, 43–59. [[CrossRef](#)]
14. Cheng, Y.; Zhang, R.; Li, T.; Zhang, F.; Russell, J.; Guan, M.; Han, Q.; Zhou, Y.; Xiao, X.; Wang, X. Spatial distributions and sources of heavy metals in sediments of the Changjiang Estuary and its adjacent coastal areas based on mercury, lead and strontium isotopic compositions. *Catena* **2019**, *174*, 154–163. [[CrossRef](#)]
15. Nakano, T.; Yamashita, K.; Ando, A.; Kusaka, S.; Saitoh, Y. Geographic variation of Sr and S isotope ratios in bottled waters in Japan and sources of Sr and S. *Sci. Total Environ.* **2020**, *704*, 135449. [[CrossRef](#)] [[PubMed](#)]
16. Lee, S.G.; Koh, D.C.; Ha, K.; Ko, K.S.; Lee, Y.S.; Jung, Y.Y.; Cheng, Z.; Chen, S.S. Geochemical Implication of Chemical Composition of Mineral Water (Bottled Water) Produced Near Mt. Baekdu (Changbai), Northeast China. *Water* **2021**, *13*, 2191. [[CrossRef](#)]
17. Shirahata, H.; Ellias, R.W.; Patterson, C.C.; Koide, M. Chronological variations in concentrations and isotopic compositions of anthropogenic atmospheric lead in sediments of a remote subalpine pond. *Geochim. Cosmochim. Acta* **1980**, *44*, 149–162. [[CrossRef](#)]
18. Elbaz-Poulichet, F.; Holliger, P.; Huang, W.W.; Martin, J.M. Lead cycling in estuaries, illustrated by the Gironde estuary, France. *Nature* **1984**, *308*, 409–411. [[CrossRef](#)]

19. Farmer, J.G.; Eades, L.J.; Mackenzie, A.B.; Kirika, A.; Bailey-Watts, T.E. Stable lead isotope record of lead pollution in Loch Lomond sediments since 1630 AD. *Environ. Sci. Technol.* **1996**, *30*, 3080–3083. [[CrossRef](#)]
20. Monna, F.; Dominik, J.; Loizeau, J.L.; Pardos, M.; Arpagaus, P. Origin and Evolution of Pb in Sediments of Lake Geneva (Switzerland-France). Establishing a Stable Pb Record. *Environ. Sci. Technol.* **1999**, *33*, 2850–2857. [[CrossRef](#)]
21. Townsend, A.T.; Snape, I. The use of Pb isotope ratios determined by magnetic sector ICP-MS for tracing Pb pollution in marine sediments near Casey Station, East Antarctica. *J. Anal. At. Spectrom.* **2002**, *17*, 922–928. [[CrossRef](#)]
22. Shotyk, W.; Weiss, D.J.; Appleby, P.G.; Cheburkin, A.K.; Frei, R.; Gloor, M.; Kramers, J.D.; Reese, S.; Van Der Knaap, W.O. History of atmospheric lead deposition since 12,370 <sup>14</sup>C yr BP from a peat bog, Jura Mountains, Switzerland. *Science* **1998**, *281*, 1635–1640. [[CrossRef](#)]
23. Weiss, D.; Shotyk, W.; Appleby, P.G.; Kramers, J.D.; Cheburkin, A.K. Atmospheric Pb deposition since the industrial revolution recorded by five Swiss peat profiles: Enrichment factors, fluxes, isotopic composition, and sources. *Environ. Sci. Technol.* **1999**, *33*, 1340–1352. [[CrossRef](#)]
24. Novák, M.; Emmanuel, S.; Vile, M.A.; Erel, Y.; Véron, A.; Paces, T.; Wieder, R.K.; Vanecek, M.; Stepanova, M.; Brizova, E.; et al. Origin of lead in eight Central European peat bogs determined from isotope ratios, strengths, and operation times of regional pollution sources. *Environ. Sci. Technol.* **2003**, *37*, 437–445. [[CrossRef](#)] [[PubMed](#)]
25. Rosman, K.J.R.; Chisholm, W.; Boutron, C.F.; Candelone, J.P.; Goerlach, U. Isotopic evidence for the source of lead in Greenland snows since the late 1960s. *Nature* **1993**, *362*, 333–335. [[CrossRef](#)] [[PubMed](#)]
26. Simonetti, A.; Gariépy, C.; Carignan, J. Pb and Sr isotopic compositions of snowpack from Québec, Canada: Inferences on the sources and deposition budgets of atmospheric heavy metals. *Geochim. Cosmochim. Acta* **2000**, *64*, 5–20. [[CrossRef](#)]
27. Walraven, N.; van Os, B.J.H.; Klaver, G.T.; Baker, J.H.; Vriend, S.P. Trace element concentrations and stable lead isotopes in soils as tracers of lead pollution in Graft-De Rijp, The Netherlands. *J. Geochem. Explor.* **1997**, *59*, 47–58. [[CrossRef](#)]
28. Hansmann, W.; Köppel, V. Lead-isotopes as tracers of pollutants in soils. *Chem. Geol.* **2000**, *171*, 123–144. [[CrossRef](#)]
29. Marcantonio, F.; Flowers, G.; Thien, L.; Ellgaard, E. Lead isotopes in tree rings: Chronology of pollution in Bayou Trepagnier, Louisiana. *Environ. Sci. Technol.* **1998**, *32*, 2371–2376. [[CrossRef](#)]
30. Watmough, S.A.; Hughes, R.J.; Hutchinson, T.C. <sup>206</sup>Pb/<sup>207</sup>Pb Ratios in Tree Rings as Monitors of Environmental change. *Environ. Sci. Technol.* **1999**, *33*, 670–673. [[CrossRef](#)]
31. Patrick, G.J.; Farmer, J.G. A stable lead isotopic investigation of the use of sycamore tree rings as a historical biomonitor of environmental lead contamination. *Sci. Total Environ.* **2006**, *362*, 278–291. [[CrossRef](#)]
32. Carignan, J.; Gariépy, C. Isotopic composition of epiphytic lichens as a tracer of sources of atmospheric lead emissions in southern Québec, Canada. *Geochim. Cosmochim. Acta* **1995**, *59*, 4427–4433. [[CrossRef](#)]
33. Monna, F.; Aiuppa, A.; Varrica, D.; Dongarra, G. Pb isotope composition in lichens and aerosols from eastern Sicily: Insights into the regional impact of volcanoes on the environment. *Environ. Sci. Technol.* **1999**, *33*, 2517–2523. [[CrossRef](#)]
34. Doucet, F.J.; Carignan, J. Atmospheric Pb isotopic composition and trace metal concentration as revealed by epiphytic lichens: An investigation related to two altitudinal sections in Eastern France. *Atmos. Environ.* **2001**, *35*, 3681–3690. [[CrossRef](#)]
35. Cloquet, C.; Carignan, J.; Libourel, G. Atmospheric pollutant dispersal around an urban area using trace metal concentrations and Pb isotopic compositions in epiphytic lichens. *Atmos. Environ.* **2006**, *40*, 574–587. [[CrossRef](#)]
36. Kylander, M.E.; Weiss, D.J.; Jeffries, T.E.; Kober, B.; Dolgoplova, A.; Garcia-Sanchez, R.; Coles, B.J. A rapid and reliable method for Pb isotopic analysis of peat and lichens by laser ablation-quadrupole-inductively coupled plasma-mass spectrometry for biomonitoring and sample screening. *Anal. Chim. Acta* **2007**, *582*, 116–124. [[CrossRef](#)] [[PubMed](#)]
37. Makishima, A. *Thermal Ionization Mass Spectrometry (TIMS): Silicate Digestion, Separation, and Measurement*; John Wiley & Sons, Inc: Weinheim, Germany, 2016; p. 339.
38. Ehrlich, S.; Gavrieli, I.; Dor, L.B.; Halicz, L.J. Direct high-precision measurements of the <sup>87</sup>Sr/<sup>86</sup>Sr isotope ratio in natural water, carbonates and related materials by multiple collector inductively coupled plasma mass spectrometry (MC-ICP-MS). *J. Anal. At. Spectrom.* **2001**, *16*, 1389–1392. [[CrossRef](#)]
39. Yang, Y.H.; Wu, F.Y.; Xie, L.W.; Yang, J.H.; Zhang, Y.B. High-precision direct determination of the <sup>87</sup>Sr/<sup>86</sup>Sr isotope ratio of bottled Sr-rich natural mineral drinking water using multiple collector inductively coupled plasma mass spectrometry. *Spectrochim. Acta Part B* **2011**, *66*, 656–660. [[CrossRef](#)]
40. Li, C.F.; Guo, J.H.; Chu, Z.Y.; Feng, L.J.; Wang, X.C. Direct high-precision measurements of the <sup>87</sup>Sr/<sup>86</sup>Sr isotope ratio in natural water without chemical separation using thermal ionization mass spectrometry equipped with 10<sup>12</sup> Ω resistors. *Anal. Chem.* **2015**, *87*, 7426–7432. [[CrossRef](#)] [[PubMed](#)]
41. Raczek, I.; Jochum, K.P.; Hofmann, A.W. Neodymium and strontium isotope data for USGS reference materials BCR-1, BCR-2, BHVO-1, BHVO-2, AGV-1, AGV-2, GSP-1, GSP-2 and eight MPI-DING reference glasses. *Geostand. Geoanal. Res.* **2003**, *27*, 173–179. [[CrossRef](#)]
42. Lee, H.M.; Jo, H.J.; Kim, T.H. Lead isotope measurement of geological reference materials using thermal ionization mass spectrometry. *Anal. Sci. Technol.* **2020**, *33*, 245–251, (In Korean with English abstract).
43. Yokoyama, T.; Makishima, A.; Nakamura, E. Evaluation of the coprecipitation of incompatible trace elements with fluoride during silicate rock dissolution by acid digestion. *Chem. Geol.* **1999**, *157*, 175–187. [[CrossRef](#)]
44. Lee, H.M. Geochemical and isotopic characteristics of the Pirrit Hills granite in West Antarctica. Ph.D. Thesis, Kongju National University, South Korea, 2013.

45. Lee, H.M.; Lee, S.G.; Tanaka, T. The effect of eluent concentration on the separation of Nd with Ln-resin method. *J. Petrol. Soc. Korea* **2015**, *24*, 365–371, (In Korean with English abstract). [[CrossRef](#)]
46. Stein, M.; Starinsky, A.; Katz, A.; Glodstein, S.L.; Machlus, M.; Schramm, A. Strontium isotopic, chemical, and sedimentological evidence for the evolution of Lake Lisan and the Dead Sea. *Geochim. Cosmochim. Acta* **1997**, *61*, 3975–3992. [[CrossRef](#)]
47. Yuan, H.; Yuan, W.; Cheng, C.; Liang, P.; Liu, X.; Dai, M.; Bao, Z.; Zong, C.; Chen, K.; Lai, S. Evaluation of lead isotope compositions of NIST NBS 981 measured by thermal ionization mass spectrometer and multiple-collector inductively coupled plasma mass spectrometer. *Solid Earth Sci.* **2016**, *1*, 74–78. [[CrossRef](#)]
48. Tanaka, R.; Makishima, A.; Kitagawa, H.; Nakamura, E. Suppression of Zr, Nb, Hf and Ta coprecipitation in fluoride compounds for determination in Ca-rich materials. *J. Anal. At. Spectrom.* **2003**, *18*, 1458–1463. [[CrossRef](#)]
49. Pretorius, W.; Weis, D.; Williams, G.; Hanano, D.; Kieffer, B.; Scoates, J. Complete trace elemental characterisation of granitoid (USGS G-2, GSP-2) reference materials by high resolution inductively coupled plasma-mass spectrometry. *Geostand. Geoanal. Res.* **2006**, *30*, 39–54. [[CrossRef](#)]
50. Retzmann, A.; Zimmermann, T.; Pröfrock, D.; Prohaska, T.; Irrgeher, J. A fully automated simultaneous single-stage separation of Sr, Pb, and Nd using DGA Resin for the isotopic analysis of marine sediments. *Anal. Bioanal. Chem.* **2017**, *409*, 5463–5480. [[CrossRef](#)] [[PubMed](#)]
51. Nath, B.N.; Makishima, A.; Noordmann, J.; Tanaka, R.; Nakamura, E. Comprehensive analysis for major, minor and trace element contents and Sr-Nd-Pb-Hf isotope ratios in sediment reference materials, JSd-1 and MAG-1. *Geochem. J.* **2009**, *43*, 207–216. [[CrossRef](#)]
52. Chauvel, C.; Bureau, S.; Poggi, C. Comprehensive chemical and isotopic analyses of basalt and sediment reference materials. *Geostand. Geoanal. Res.* **2011**, *35*, 125–143. [[CrossRef](#)]
53. Lee, H.M.; Lee, S.G.; Tanaka, T.; Lee, S.R. Determination of Sr, Nd isotope ratios of standard rock samples using thermal ionization mass spectrometer (TIMS). In Proceedings of the Fall Conference of the Korean Association of Analytical Sciences, JeJu, Korea, 20 November 2014.
54. Klaver, M.; Djuly, T.; de Graaf, S.; Sakes, A.; Wijbrans, J.; Davies, G.; Vroon, P. Temporal and spatial variations in provenance of Eastern Mediterranean Sea: Implications for Aegean and Aeolian arc volcanism. *Geochim. Cosmochim. Acta* **2015**, *153*, 149–168. [[CrossRef](#)]
55. Révillon, S.; Hureau-Mazaudier, D. Improvements in digestion protocols for trace element and isotope determinations in stream and lake sediment reference materials (JSd-1, JSd-2, JSd-3, JLk-1 and LKSD-1). *Geoanal. Res.* **2009**, *33*, 397–413. [[CrossRef](#)]
56. Saitoh, Y.; Ishikawa, T.; Tanimizu, M.; Murayama, M.; Ujiie, Y.; Yamamoto, Y.; Ujiie, K.; Kanamatsu, T. Sr, Nd, and Pb isotope compositions of hemipelagic sediment in the Shikoku Basin: Implications for sediment transport by the Kuroshio and Philippine Sea plate motion in the late Cenozoic. *Earth Planet. Sci. Lett.* **2015**, *421*, 47–57. [[CrossRef](#)]
57. Li, C.F.; Wang, X.C.; Guo, J.H.; Chu, Z.Y.; Feng, L.J. Rapid separation scheme of Sr, Nd, Pb, and Hf from a single rock digest using a tandem chromatography column prior to isotope ratio measurements by mass spectrometry. *J. Anal. At. Spectrom.* **2016**, *31*, 1150–1159. [[CrossRef](#)]
58. Ackerman, L.; Magna, T.; Rapprich, V.; Upadhyay, D.; Krátký, O.; Čejková, B.; Erban, V.; Kochergina, Y.U.V.; Hrstka, T. Contrasting petrogenesis of spatially related carbonatites from Samalpatti and Sevattur, Tamil Nadu, India. *Lithos* **2017**, *284–285*, 257–275. [[CrossRef](#)]